5066 *Biochemistry* **2010,** *49,* 5066–5073
DOI: 10.1021/bi100272g

BIOCHEMISTRY
including biophysical chemistry & molecular biology
Article

Insights into the Mechanism of *Pseudomonas dacunhae* Aspartate β-Decarboxylase from Rapid-Scanning Stopped-Flow Kinetics

Robert S. Phillips,*[,‡,§] Santiago Lima,[§] Roman Khristoforov,[‡] and Bakthavatsalam Sudararaju[‡]

[‡]*Department of Chemistry, University of Georgia, Athens, Georgia 30602, and* [§]*Department of Biochemistry and Molecular Biology, University of Georgia, Athens, Georgia 30602*

Received February 23, 2010; Revised Manuscript Received May 14, 2010

ABSTRACT: The mechanism of wild-type and R37A mutant *Pseudomonas dacunhae* aspartate β-decarboxylase (ABDC) was studied by rapid-scanning stopped-flow spectrophotometry. Mixing wild-type ABDC with 50 mM disodium L-Asp resulted in the formation of a 325 nm absorption peak within the dead time of the stopped-flow instrument, likely the ketimine of pyridoxamine 5′-phosphate and oxaloacetate or pyruvate. After consumption of the L-Asp, the 360 nm feature of the resting enzyme was restored. Thus, the 325 nm species is a catalytically competent intermediate. In contrast, mixing wild-type ABDC with the disodium salt of either *threo*- or *erythro*-β-hydroxy-DL-Asp at 50 mM resulted in a much slower formation of the 325 nm complex, with an apparent rate constant of ∼1 or 0.006 s^{-1}, respectively. When wild-type ABDC is mixed with disodium succinate, a nonreactive analogue of L-Asp, formation of a new peak at 425 nm is observed. The apparent rate constant for formation of the 425 nm band exhibits a hyperbolic dependence on succinate concentration, showing that there is a rapid binding equilibrium, followed by a slower reaction in which the internal aldimine is protonated on the Schiff base N. Hydrostatic pressure shifts the spectrum from the 425 nm form to the 360 nm form, consistent with a conformational change. It is likely that the binding of substrate or analogues induces a conformational change that releases strain in the Lys pyridoxal 5′-phosphate Schiff base and increases the pK_a, resulting in protonation of the Schiff base to initiate transaldimination. Mixing of R37A mutant ABDC with 50 mM L-Asp also results in the formation of the 325 nm complex, but with an apparent rate constant of 0.2 s^{-1}, at least 5000-fold slower than the rate of wild-type ABDC. In contrast to wild-type ABDC, R37A ABDC shows no change in the cofactor spectrum when mixed with disodium succinate. These results suggest that Arg-37, a conserved active site residue in ABDC, plays a role in modulating the pK_a of the pyridoxal 5′-phosphate complexes during catalysis.

Aspartate β-decarboxylase (ABDC)[1] is a pyridoxal 5′-phosphate (PLP)-dependent enzyme found mainly in bacteria (*1*), although it has also been reported in mammalian tissues (*2*). ABDC catalyzes the irreversible β-decarboxylation of L-aspartate to give L-alanine and carbon dioxide (eq 1)

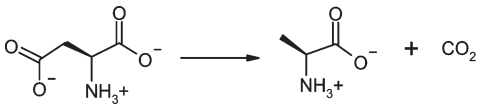

(1)

In bacteria, this reaction is coupled with an Asp/Ala antiporter in the cell membrane, resulting in a proton gradient and net ATP synthesis (*3*). The mechanism of ABDC is intriguing, since it is the only known PLP-dependent enzyme that catalyzes β-decarboxylation, rather than α-decarboxylation.

Recently, the three-dimensional structures of *Pseudomonas dacunhae* and *Alcaligenes faecalis* ABDC were determined by X-ray crystallography (*4*, *5*). The enzyme exists as a dodecameric quaternary structure unique among the members of the PLP-dependent aminotransferase family, most of which form dimers or tetramers. However, despite these quaternary structural differences, the active site of ABDC is remarkably similar to that of aspartate aminotransferase (AAT) (*4*). One notable difference between the structure of ABDC and AAT is the presence of an additional arginine residue, Arg-37, in the active site, which is conserved in all known ABDC sequences. We previously prepared the mutant R37A ABDC and found that it retains significant activity, apparently ruling out a role for Arg-37 as an essential active site acid−base catalyst (*4*). We have now examined the pre-steady state kinetics of the reactions of wild-type and R37A mutant ABDC with L-Asp, *erythro*- and *threo*-β-hydroxy-DL-Asp, and succinate. These results suggest that Arg-37 plays an important role in modulating the ionization state of the PLP cofactor during catalysis.

MATERIALS AND METHODS

Enzymes. Recombinant wild-type and R37A ABDC from *P. dacunhae* were prepared as previously described (*4*). Enzyme assays were performed using a coupled assay with alanine dehydrogenase as previously described (*4*), measuring the increase in absorbance at 340 nm ($\Delta\varepsilon$ = 6200 M^{-1} cm^{-1}) as NAD^+ is converted to NADH.

Materials. L-Aspartate was a product of Sigma-Aldrich Chemical Co. Succinic acid was obtained from Fisher Scientific.

*To whom correspondence should be addressed: Department of Chemistry, University of Georgia, Athens, GA 30602. Phone: (706) 542-1996. Fax: (706) 542-9454. E-mail: rsphillips@chem.uga.edu.

[1]Abbreviations: ABDC, aspartate β-decarboxylase; AAT, aspartate aminotransferase; PLP, pyridoxal 5′-phosphate; PMP, pyridoxamine 5′-phosphate; β-hydroxyAsp, β-hydroxy-DL-aspartic acid.

 Published on Web 05/14/2010

Threo- and *erythro-β*-hydroxy-DL-Asp (*6*) were generous gifts of C. H. Stammer. Other common chemicals were obtained from Fisher Scientific.

Instruments. Stopped-flow kinetics experiments were performed on an RSM-1000 instrument from OLIS, Inc. (Bogart, GA), equipped with a stopped-flow cell compartment. This instrument has a dead time of ca. 2 ms and can collect UV−visible scans at speeds up to 1000 Hz. The stopped-flow experiments were performed at ambient temperature, generally 22−25 °C. The enzyme assays were performed on a Cary 1 UV−visible spectrophotometer equipped with a Peltier-controlled six-cell changer. The effects of hydrostatic pressure on the absorption spectra of the ABDC−succinate complex were measured using a Cary 14 UV−vis spectrophotometer modified by OLIS, Inc., to contain a high-pressure cell from ISS (Champaign, IL), equipped with a manual pressure pump, and maintained at 25 °C with an external circulating water bath.

Stopped-Flow Experiments. The stopped-flow experiments were performed in 0.1 M sodium acetate buffer (pH 6.0). The enzyme was exchanged into the reaction buffer by rapid gel filtration on a PD-10 column (GE Corp.) equilibrated with 0.1 M sodium acetate (pH 6.0) immediately before use. Solutions of wild-type or R37A mutant ABDC (2−3.2 mg/mL) were mixed with disodium salts of L-Asp, *erythro-* or *threo-β*-hydroxyAsp (0.1 M), or various concentrations of disodium succinate (0.02−0.3 M). We prepared the disodium salts by dissolving the acids in 2 equiv of 1 M NaOH before dilution with acetate buffer. Scans were collected from 250 to 800 nm for various periods of time and scanning rates after mixing, depending on the rate of the individual reaction monitored. The stopped-flow data were analyzed using Global Works (*7*) provided by OLIS, Inc. The data were fitted to models of either one or two exponentials as necessary to obtain reasonable fits. The concentration dependence for reactions of succinate was fitted to eq 2

$$K_{obs} = (k_f[\text{succinate}])/(K_{eq} + [\text{succinate}]) + k_r \qquad (2)$$

where K_{eq} is the dissociation constant, k_f is the rate constant for the forward reaction, and k_r is the rate constant for the reverse reaction (*8*).

Hydrostatic Pressure Experiments. The enzyme solution contained 1 mg/mL ABDC in 0.1 M MES-Na^+ (pH 5.3) containing 0.1 M disodium succinate in 1.2 mL quartz bottles with a 9 mm path length, capped with Teflon tubing and immersed in spectroscopic-grade ethanol as the pressurizing fluid. MES buffer was used rather than acetate since buffers with anionic conjugate bases have a high ΔpK_a with pressure (*9*). A buffer blank containing 0.1 M MES-Na^+ (pH 5.3) and 0.1 M disodium succinate at 100 bar was used to obtain a baseline reading. The pressure was increased or decreased in 100 bar increments to a maximum of 1900 bar, and the enzyme solutions were scanned immediately after each increase or decrease in pressure. The total time to measure the spectra through the range of increasing and decreasing pressures was approximately 2 h. Absorbance values at 425 nm were corrected for solvent compressibility using a modified Tait equation (*10*). The corrected absorbance values were analyzed by fitting to eq 3

$$A_P = (A_\infty - A_o)[K_{eq} \times \exp(-P\Delta V_o/RT)]/[1 + K_{eq} \times \exp(-P\Delta V_o/RT)] + A_\infty \qquad (3)$$

where A_P is the observed absorbance at pressure P, A_o is the absorbance at 0 bar, A_∞ is the absorbance at infinite pressure, K_{eq} is the pressure-independent value of the apparent equilibrium constant, and ΔV_o is the reaction volume.

RESULTS

Reaction of Wild-Type ABDC with L-Aspartate. When wild-type ABDC is mixed with 50 mM disodium L-Asp in the stopped-flow spectrophotometer, there is a rapid change in the spectrum within the dead time of the instrument, ca. 2 ms, from the 360 nm form of the resting enzyme to a spectrum with peaks at 325 and 360 nm and a small shoulder at 425 nm (spectrum 1, Figure 1A). As the Asp substrate is consumed, in ∼1 min, the spectrum gradually reverts to one similar to that of the resting form, with a λ_{max} of 360 nm (Figure 1A,B).

Reaction of Wild-Type ABDC with threo- and erythro-β-Hydroxy-DL-aspartate. Mixing wild-type ABDC with 50 mM disodium *threo-β*-hydroxy-DL-Asp results in a slow reaction, with formation of a spectrum with a peak at 325 nm, a shoulder at 360 nm, and a very weak shoulder at 430 nm (Figure 2A) that resembles the spectrum formed with L-Asp. There is an isosbestic point in the spectra at 335 nm. In contrast to the reaction with L-Asp, these spectroscopic changes take place over 3 s (Figure 2B), with a rate constant of ∼1 s^{-1}. Since the reaction with L-Asp occurs within the dead time of the stopped-flow instrument (≤2 ms), the corresponding reaction with L-Asp must occur with a rate constant greater than 1000 s^{-1}.[2] Thus, the reaction of *threo-β*-hydroxy-DL-Asp with ABDC is at least 1000-fold slower than that with L-Asp. The reaction with 50 mM disodium *erythro-β*-hydroxy-DL-Asp produces a spectrum similar to those of L-Asp and *threo-β*-hydroxy-DL-Asp, with an absorbance peak at 325 nm, a shoulder at 360 nm, and a very weak shoulder at 430 nm, albeit much more slowly, over a period of ∼3 min, with a rate constant of ∼0.006 s^{-1} (Figure 2C,D). This shows that the reaction of *erythro-β*-hydroxy-DL-Asp with ABDC is at least 16700-fold slower than that with L-Asp.[2] These spectra also exhibit an isosbestic point at 335 nm.

Reaction of Wild-Type ABDC with Succinate. When wild-type ABDC is mixed with disodium succinate, there is a rapid decrease in the 360 nm absorbance peak and an increase in an absorbance peak at 425 nm (Figure 3A,B), with an isosbestic point at 386 nm. The apparent rate constant for the reaction is dependent on the concentration of succinate, over the range from 10 to 150 mM, with a hyperbolic dependency (Figure 4). Fitting these data to eq 2 gives the following values: $k_f = 71.6 \pm 1.2\ s^{-1}$, $k_r = 37.3 \pm 1.5\ s^{-1}$, and $K_{eq} = 21.9 \pm 1.7$ mM.

When the ABDC−succinate complex is subjected to increasing hydrostatic pressure, the spectrum shifts, with a decrease in the 425 nm absorbance and an increase in the 360 nm absorbance, and with an isosbestic point at 386 nm (Figure 5A), so there are only two absorbing species contributing to the spectra. The absorbance change at 425 nm with pressure is shown in Figure 6B, with the empty circles indicating the data obtained during the compression and the filled circles the corresponding data obtained during decompression. These data show that the changes in the spectrum with pressure are completely reversible, indicating that there is a simple reversible equilibrium between the two states. Fitting the 425 nm data in Figure 5B to eq 3 gives

[2]The reaction of ABDC with L-Asp is over within the dead time of the stopped-flow instrument, which is ∼2 ms. Assuming that the reaction is not seen because at least three half-lives have passed in the dead time, the half-life would then be less than 0.67 ms. The lower limit on the rate constant is then given by $0.693/6.7 \times 10^{-4}\ s = 1034\ s^{-1}$.

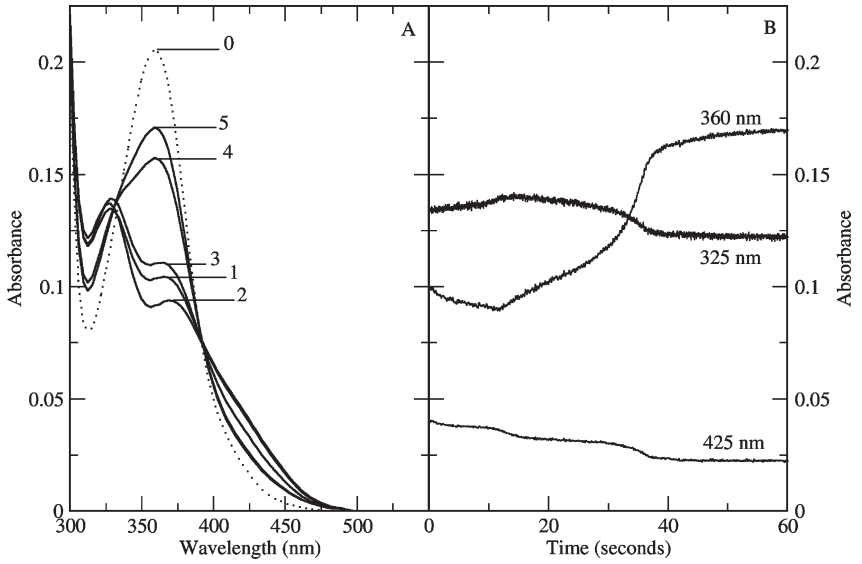

FIGURE 1: Reaction of wild-type ABDC with 50 mM disodium L-Asp in 0.1 M sodium acetate (pH 6.0). (A) Scans are shown at 0.002, 2.69, 8.9, 37.1, and 60.5 s. The dotted line (spectrum 0) is the spectrum of the enzyme before the reaction. (B) Time courses at 360 and 425 nm.

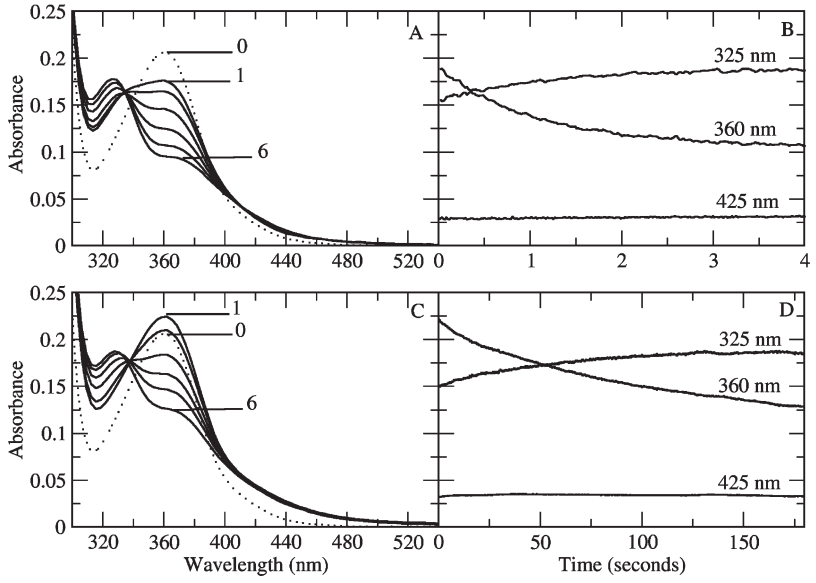

FIGURE 2: (A) Reaction of wild-type ABDC with 50 mM disodium *threo*-β-hydroxy-DL-Asp in 0.1 M sodium acetate (pH 6.0). Scans are shown at 0.0087, 0.249, 0.601, 1.19, 2.38, and 5.31 s. The dotted line (spectrum 0) is the spectrum of the enzyme before the reaction. (B) Time courses for the reaction of *threo*-β-hydroxy-DL-Asp at 360 and 425 nm. (C) Reaction of wild-type ABDC with 50 mM disodium *erythro*-β-hydroxy-DL-Asp in 0.1 M sodium acetate (pH 6.0). Scans are shown at 0.411, 7.19, 35.9, 71.8, 107.7, and 179.7 s. The dotted line (spectrum 0) is the spectrum of the enzyme before the reaction. (D) Time courses for the reaction of *erythro*-β-hydroxy-DL-Asp at 360 and 425 nm.

the following values: $K_{eq} = 0.0169 \pm 0.0072$, and $\Delta V = -50 \pm 20$ mL/mol.

Reaction of R37A ABDC with L-Asp and Succinate. Mixing R37A ABDC with 50 mM disodium L-Asp results in a slow decrease in the magnitude of the 360 nm absorption peak, concomitant with an increase at 330 nm (Figure 6A,B). The absorbance changes take ~10 s to complete, with an apparent rate constant of ~0.2 s^{-1}. Thus, the reaction of R37A ABDC is ~5000-fold slower than that with wild-type ABDC.[2] In contrast to wild-type ABDC, there is no significant shoulder at 425 nm in the spectra. Mixing R37A ABDC with 100 mM disodium succinate results in no significant change in the spectrum (data not shown).

DISCUSSION

ABDC catalyzes the β-decarboxylation of L-Asp to give L-Ala and CO_2 (*1*). This reaction is the only known PLP-dependent β-decarboxylation reaction, and there are only a few PLP-dependent enzymes that catalyze similar reactions involving $\beta-\gamma$ bond cleavage with resulting electrophilic rather than nucleophilic substitution at the β-carbon, including kynureninase (*11*), cysteine desulfurase (*12*), and selenocysteine lyase (*13*). It has been suggested that these enzymes utilize PMP-ketimine intermediates to polarize the $\beta-\gamma$ bond and provide an electron sink for the reaction forming a formal β-carbanion (*11*−*13*). PMP-ketimine intermediates are also commonly found in aminotransferase reactions and generally exhibit absorption peaks at ~325 nm arising from the PMP (*14*). Novogrodsky and Meister reported that a 325 nm complex is formed in the steady state from ABCD and L-Asp, but they assumed that it was the result of the abortive transamination resulting in PMP and oxaloacetate (*15*). In our work, we find that mixing ABDC with L-Asp results in the formation of a 325 nm intermediate within the dead time of the

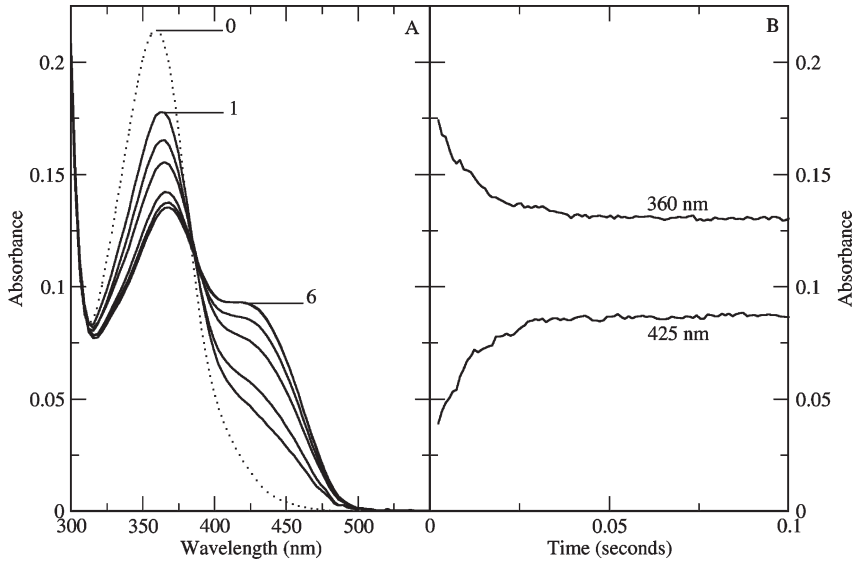

FIGURE 3: Reaction of wild-type ABDC with 100 mM disodium succinate in 0.1 M sodium acetate (pH 6.0). (A) Scans are shown at 0.0055, 0.0105, 0.0175, 0.0265, 0.0405, and 0.0995 s. The dotted line (spectrum 0) is the spectrum of the enzyme before the reaction. (B) Time courses at 360 and 425 nm.

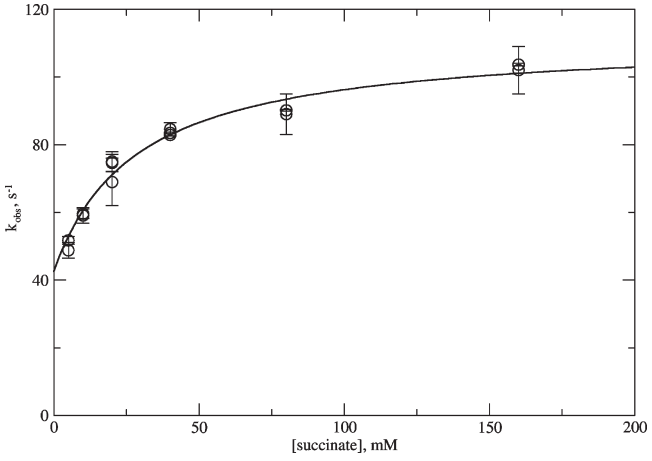

FIGURE 4: Dependence of the rate constant for the reaction of wild-type ABDC with disodium succinate. The curve is calculated from fitting of the data to eq 2 with the following values: $k_f = 71.6\ s^{-1}$, $k_r = 37.3\ s^{-1}$, and $K_{eq} = 21.9$ mM.

stopped-flow instrument (Figure 1). This intermediate spectrum remains constant during the steady state, but the spectrum rapidly reverts back to the resting 360 nm form when substrate is depleted (Figure 1). This result suggests that the 325 nm species is a catalytically competent intermediate rather than a branch species arising from abortive transamination. It is reasonable to assign the structure of the 325 nm species formed from ABDC and Asp to a PMP-ketimine, either with oxaloacetate, before decarboxylation, or with pyruvate, after decarboxylation. Since ^{13}C isotope effects indicated that decarboxylation is not rate-limiting (*16*), it seems more likely that the 325 nm complex in the steady state is the ketimine of pyruvate with PMP.

Miles and Meister studied the reaction of ABDC with the *threo* and *erythro* diastereomers of β-hydroxyAsp, and they found that both isomers are slow substrates, undergoing β-decarboxylation at ~0.02% of the rate of L-Asp to form L-Ser (*17*). These authors also noticed formation of a transient complex absorbing at 325 nm with both diastereomers of β-hydroxyAsp. The 325 nm complex of β-hydroxyAsp is stable enough to be isolated by gel filtration, and it decays slowly to release L-Ser (*17*). Thus, the 325 nm complex is also catalytically competent for the reactions of β-hydroxyAsp. In our studies, we also found that the 325 nm species is formed from the β-hydroxyAsp diastereomers, albeit much more slowly than from L-Asp (Figure 2). However, *threo*-β-hydroxyAsp reacts 167-fold faster than the *erythro* isomer (Figure 2) to form the 325 nm complex. This is consistent with the much weaker binding of the *erythro* diastereomer reported by Miles and Meister (*17*). A proposed mechanism for the reaction of the β-hydroxyAsp diastereomers with ABDC is shown in Scheme 1. Formation of an external aldimine is followed by deprotonation to a quinonoid intermediate, which is then reprotonated to give a β-hydroxyoxaloacetate ketimine of PMP. Decarboxylation would give an enolamine, which is reprotonated on the β-carbon to give a β-hydroxypyruvate ketimine. Deprotonation of this ketimine at C-4′ gives the serine quinonoid intermediate which is reprotonated at α-C to give the external aldimine of L-Ser, which releases L-Ser. The very slow formation of the ketimine from the β-hydroxyAsp residues suggests that either the external aldimine formation or the aldimine−ketimine interconversion is slow. Miles and Meister were surprised by the stability of the 325 nm intermediate formed from β-hydroxyAsp residues and proposed that either a protein nucleophile formed an adduct with the L-Ser aldimine or an oxazolidine was formed by intramolecular addition of the β-hydroxy group of the nascent L-Ser to the aldimine (*17*). Since L-Asp forms a similar transient intermediate from either diastereomer of β-hydroxyAsp, we believe it is more likely that the 325 nm species is a relatively stable ketimine. An alternative explanation for the stability of the complex is that it is an enolamine formed subsequent to β-decarboxylation, which may be only slowly reprotonated on the β-carbon because of either steric effects or altered electronics (Scheme 1). It is interesting in this regard that *threo*-β-hydroxyAsp is a normal substrate for AAT, while *erythro*-β-hydroxyAsp forms a quasi-stable quinonoid complex that turns over very slowly (*18*). Since the active sites of ABDC and AAT are nearly identical in structure (*4*), it seems likely that there are similar interactions of the β-hydroxyAsp diastereomers in both active sites. The structure of the quinonoid complex of

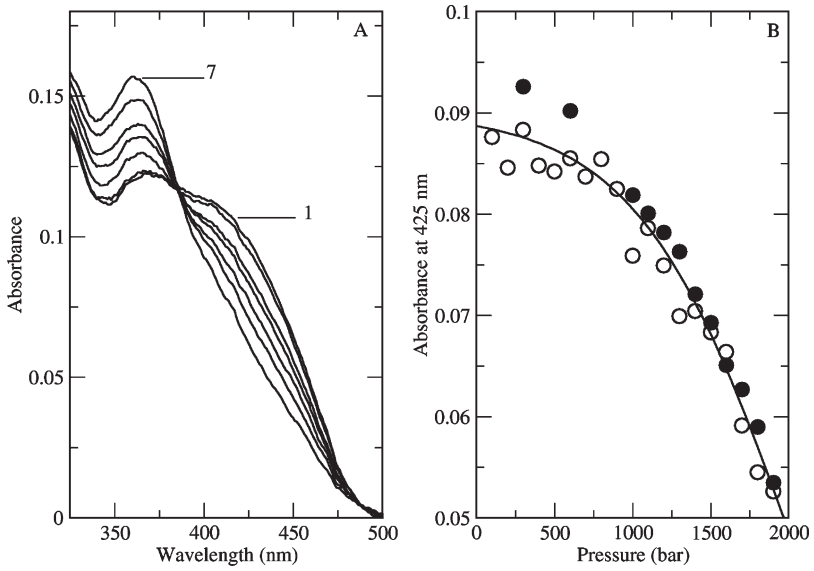

FIGURE 5: Effect of hydrostatic pressure on the ABDC−succinate complex. The solution contained ABDC (1 mg/mL), 0.1 M MES (pH 5.3), and 0.1 M disodium succinate. (A) Spectra are shown at (1) 300, (2) 600, (3) 1100, (4) 1300, (5) 1500, (6) 1700, and (7) 1900 bar. (B) Absorbance at 425 nm of the ABDC−succinate complex at various pressures: (○) increasing pressure and (●) decreasing pressure. The line through the points is the result of fitting the data to eq 3.

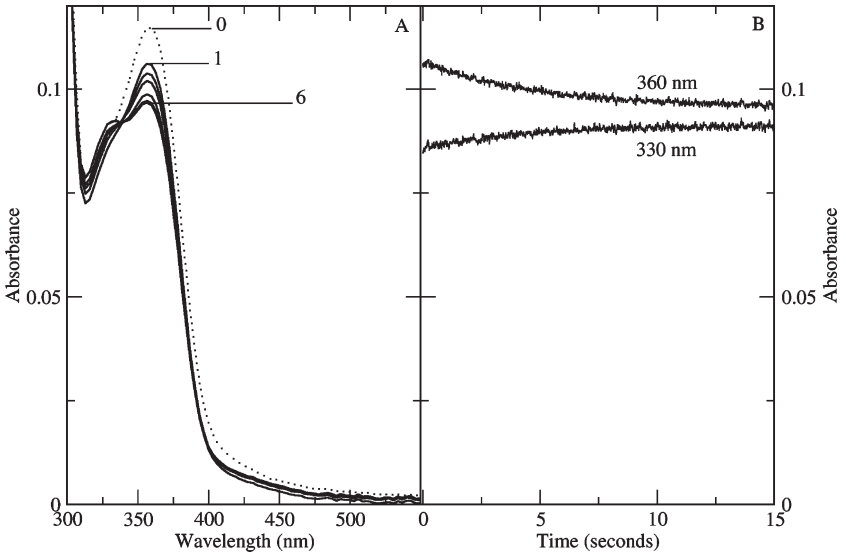

FIGURE 6: Reaction of R37A ABDC with 50 mM disodium L-Asp in 0.1 M sodium acetate (pH 6.0). (A) Scans are shown at 0.005, 3.08, 5.49, 9.05, and 15.80 s. The dotted line (spectrum 0) is the spectrum of the enzyme before the reaction. (B) Time courses at 360 and 425 nm.

erythro-β-hydroxyAsp with AAT shows a hydrogen bond between Tyr-70 and the β-OH group of the β-hydroxyAsp (*19*). Mutation of Tyr-70 to Phe in AAT reduces the affinity of *erythro*-β-hydroxyAsp and destabilizes the quinonoid complex, showing that the hydrogen bond contributes significantly to binding (*20*). In ABDC, the much weaker binding and slower reaction of *erythro*-β-hydroxyAsp suggest that the hydrogen bond to Tyr-134 (homologous to Tyr-70 in AAT) is not able to form, and there may be a steric clash.

Reaction of ABDC with succinate, an unreactive Asp analogue lacking the α-amino group, results in the formation of an absorption peak at 425 nm, corresponding to a protonated ketoenamine tautomer of the PLP-lysine Schiff base, from the 360 nm resting enzyme (Figure 3). The rate constant for this reaction is a function of succinate concentration, with a hyperbolic dependency (Figure 4). This result demonstrates that there is rapid equilibrium binding of succinate, followed by a slower reaction in which the PLP becomes partially protonated on the PLP-lysine Schiff base (eq 4).

$$\mathrm{E(360\ nm) + succinate} \overset{K=21.9\ \mathrm{mM}}{\rightleftharpoons}$$

$$\mathrm{E\cdot succinate(360\ nm)} \underset{k_r=37.3\ s^{-1}}{\overset{k_f=71.6\ s^{-1}}{\rightleftharpoons}} \mathrm{E\cdot succinate(425\ nm)} \quad (4)$$

A similar change in the PLP spectrum was observed with noncovalent ligand binding to *Escherichia coli* AAT (*21*) and was attributed to a conformational change between the open and closed states. Thus, this slow reaction of ABDC with succinate is likely a similar conformational change which changes the PLP environment and favors the protonated ketoenamine by increasing the pK_a of the aldimine N (Scheme 2). The succinate likely binds by forming salt bridges to Arg-375 and Arg-497 (Scheme 2), which are homologous with the Arg residues in AAT (Arg-292 and Arg-386, respectively, in *E. coli* AAT) that

Scheme 1: Proposed Mechanism of Decarboxylation of β-HydroxyAsp by ABDC

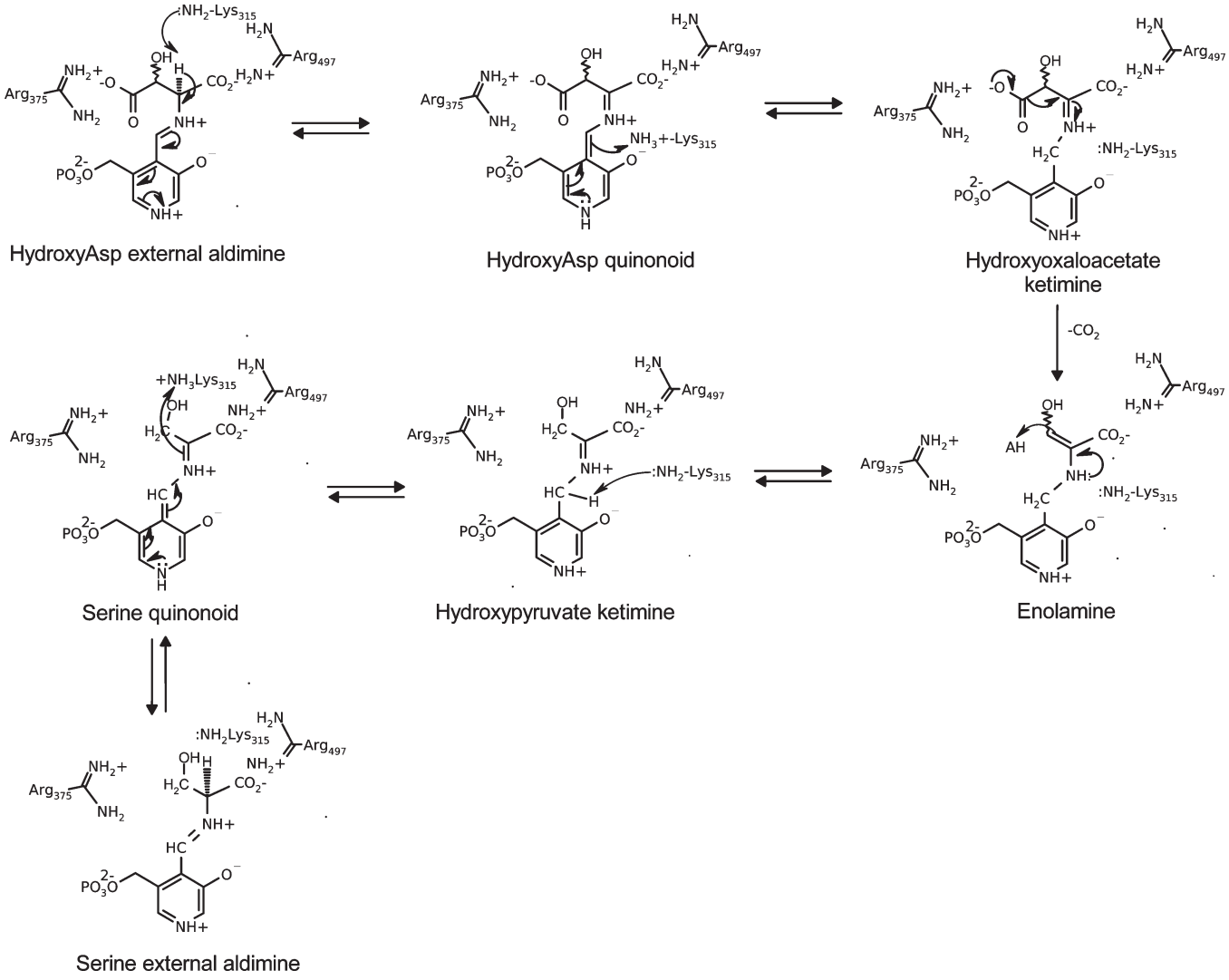

bind the α- and β-carboxylates of Asp (*22*). This hypothesis that a conformational change occurs in ABDC is supported by the effects of hydrostatic pressure on the protonation equilibrium of the succinate complex (Figure 5). In previous studies, we demonstrated that increasing hydrostatic pressure changes the allosteric equilibrium of tryptophan synthase to favor the open conformation (*23*−*25*). In this study, the 425 nm absorption shoulder of the protonated internal aldimine of ABDC in 0.1 M succinate shifts under high pressure to the unprotonated cofactor form [360 nm (Figure 5A)]. On the basis of our work with tryptophan synthase (*23*−*25*), this species is the open state, thus confirming that ABDC must undergo a conformational change to accommodate substrate and initiate transaldimination. The observed pressure-dependent changes in the spectra are not likely to arise from subunit dissociation for the following reasons. (1) The highest pressures used in our studies (1.9 kbar) are lower than those used for subunit dissociation studies, generally greater than 2.5 kbar (*26*). (2) The isosbestic point at 386 nm in the pressure studies (Figure 5A) is the same as that seen in the stopped-flow kinetic experiments (Figure 3A), indicating that the same two spectroscopic species observed in the stopped-flow kinetic experiment are involved in the pressure-sensitive equilibrium. (3) There is no hysteresis in the data when the pressure is decreased, indicating that the spectral changes are readily and rapidly reversible (i.e., first-order) upon decompression. In contrast, subunit dissociation would result in hysteresis, with the reverse reaction obeying second-order kinetics upon decompression. The ΔV_o for the ABDC conformational equilibrium is relatively small (−50 mL/mol), much lower than that for tryptophan synthase (−125 to −200 mL/mol) (*23*) but similar to that seen for the equilibrium between the 420 and 338 nm forms of the cofactor of tryptophan indole-lyase, −38 mL/mol (*27*). Since at pH 5.3, in the presence of succinate, the equilibrium still favors the neutral imine absorbing at 360 nm (Figure 5A), the pK_a of ABDC must be ≤5.3 even in the succinate complex. In contrast, for aspartate aminotransferase, the pK_a of the unliganded internal aldimine is 6.8, and it increases to 8.8 in Michaelis complexes (*21*). In solution, the pK_a values of PLP aldimines are ∼12 (*28*). Since ABDC functions physiologically when bacteria are subjected to acidic stress, the low pK_a of the internal aldimine may be important in regulation of enzyme activity in vivo.

The structure of ABDC (*4*) shows that the geometry of the PLP-lysine Schiff base is distorted, with the lysine ε-amino group out of the plane of the PLP ring and a C−C=N bond angle of ∼152° (Figure 7), far from the ideal trigonal bond angle of 120°. The distance from ε-N of Lys-315 to 3′-O of PLP is 3.68 Å, indicating that intramolecular H-bonding would be very weak even if the N were protonated. Instead, the 3′-O of PLP is strongly

Scheme 2: Effect of Succinate on the ABDC PLP Spectrum

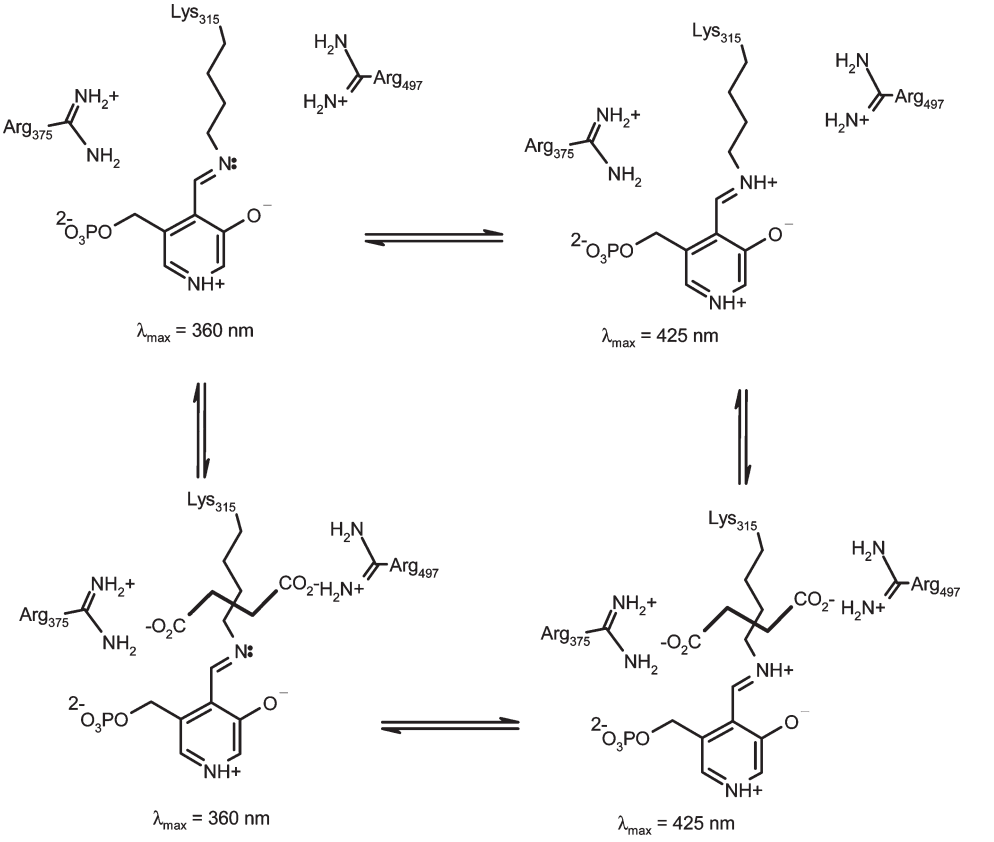

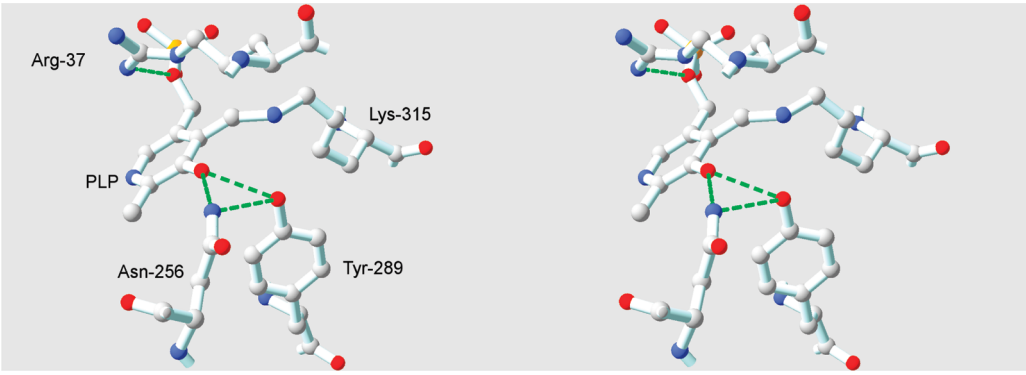

FIGURE 7: Structure of PLP in the ABDC active site. The coordinates were taken from Protein Data Bank entry 3FDD. Hydrogen bonds are represented by dashed green lines. Only heavy atoms (C, N, O, and P) are shown. This figure was prepared using SPDBV 4.01 (*29*).

H-bonded to Asn-256 and Tyr-289, with distances of ~2.8 Å (Figure 7). Arg-37 is H-bonded to the bridging O of the phosphate group of PLP (Figure 7). The protonated ketoenamine tautomer of the PLP-Lys-315 Schiff base is the one that is expected to be reactive toward transaldimination with a substrate, so a conformational change is likely to occur after L-Asp binding to activate the PLP, followed by transaldimination, which is found for AAT (*21*). Indeed, a transient shoulder at ~425 nm is observed in the reactions of L-Asp and both diastereomers of β-hydroxyAsp (Figures 1A, 2A, and 3A). However, it is interesting that R37A ABDC does not show the 425 nm shoulder in the reaction with L-Asp, and the formation of the 325 nm complex with L-Asp is ~5000-fold slower than that for wild-type ABDC (Figure 7). This very slow rate of reaction of R37A ABDC may reflect the unfavorable protonation of the internal aldimine. In fact, the rate constant for formation of the 325 nm intermediate (0.2 s^{-1}) is comparable to the steady state k_{cat} (0.7 s^{-1}) (*4*), suggesting that aldimine formation may be rate-determining for R37A ABDC. Furthermore, in contrast to wild-type ABDC, mixing of R37A ABDC with disodium succinate at pH 6 did not result in any change in the enzyme PLP spectrum (data not shown), indicating that the pK_a of the Schiff base is very low even in the succinate complex.

Conclusion. ABDC forms a PMP-ketimine intermediate during turnover with substrates. These data suggest that Arg-37 in ABDC influences the pK_a of the PLP-Lys-315 Schiff base. The electrostatic effect of this additional Arg residue in the proximity of the PLP may contribute to the low pK_a of the aldimine N in the unliganded state. However, Arg-37 also has the paradoxical effect of promoting protonation when ligands bind. Possibly, the dianionic substrate neutralizes two of the three arginine guanidinium cations and reduces the positive charge of

the active site. Arg-37 may also swing away from the cofactor to allow the substrate access. Thus, our data demonstrate that Arg-37, which is a conserved residue in ABDC, controls the protonation state, and hence the reactivity, of the PLP of ABDC, possibly by opposing the strain introduced by the H-bonds of 3′-O of PLP with Asn-256 and Tyr-289.

REFERENCES

1. Tate, S. S., and Meister, A. (1971) L-Aspartate-β-decarboxylase: Structure, catalytic activities, and allosteric regulation. *Adv. Enzymol. Relat. Areas Mol. Biol. 35*, 503–543.
2. Rathod, P. K., and Fellman, J. H. (1985) Identification of mammalian aspartate-4-decarboxylase. *Arch. Biochem. Biophys. 238*, 435–446.
3. Abe, K., Ohnishi, F., Yagi, K., Nakajima, T., Higuchi, T., Sano, M., Machida, M., Sarker, R. I., and Maloney, P. C. (2002) Plasmid-encoded asp operon confers a proton motive metabolic cycle catalyzed by an aspartate-alanine exchange reaction. *J. Bacteriol. 184*, 2906–2913.
4. Lima, S., Sundararaju, B., Huang, C., Khristoforov, R., Momany, C., and Phillips, R. S. (2009) The crystal structure of the *Pseudomonas dacunhae* aspartate-β-decarboxylase dodecamer reveals an unknown oligomeric assembly for a pyridoxal-5′-phosphate-dependent enzyme. *J. Mol. Biol. 388*, 98–108.
5. Chen, H. J., Ko, T. P., Lee, C. Y., Wang, N. C., and Wang, A. H. (2009) Structure, assembly, and mechanism of a PLP-dependent dodecameric L-aspartate β-decarboxylase. *Structure 17*, 517–529.
6. Jones, C. W., III, Leyden, D. E., and Stammer, C. H. (1969) *threo* and *erythro* β-hydroxy-DL-aspartic acids. *Can. J. Chem. 47*, 4363–4366.
7. Matheson, I. B. C. (1990) A critical comparison of least absolute deviation fitting (robust) and least-squares fitting: The importance of error distributions. *Comput. Chem. 14*, 49–57.
8. Strickland, S., Palmer, G., and Massey, V. (1975) Determination of dissociation constants and specific rate constants of enzyme-substrate (or protein-ligand) interactions from rapid reaction kinetic data. *J. Biol. Chem. 250*, 4048–4052.
9. Kitamura, Y., and Itoh, T. (1987) Reaction of protonic ionization for buffering agents. *J. Solution Chem. 16*, 715–725.
10. Li, Y.-H. (1967) Equation of state of water and sea water. *J. Geophys. Res. 72*, 2665–2678.
11. Soda, K., and Tanizawa, K. (1979) Kynureninases: Enzymological properties and regulation mechanism. *Adv. Enzymol. Relat. Areas Mol. Biol. 49*, 1–40.
12. Zheng, L., White, R. H., Cash, V. L., and Dean, D. R. (1994) Mechanism for the desulfurization of L-cysteine catalyzed by the *nif*S gene product. *Biochemistry 33*, 4714–4720.
13. Esaki, N., Karai, N., Nakamura, T., Tanaka, H., and Soda, K. (1985) Mechanism of reactions catalyzed by selenocysteine β-lyase. *Arch. Biochem. Biophys. 238*, 418–423.
14. Metzler, C. M., and Metzler, D. E. (1987) Quantitative description of absorption spectra of a pyridoxal phosphate-dependent enzyme using lognormal distribution curves. *Anal. Biochem. 166*, 313–327.
15. Novogrodsky, A., and Meister, A. (1964) Control of aspartate β-decarboxylase activity by transamination. *J. Biol. Chem. 239*, 879–888.
16. Rosenberg, R. M., and O'Leary, M. H. (1985) Aspartate β-decarboxylase from *Alcaligenes faecalis*: Carbon-13 kinetic isotope effect and deuterium exchange experiments. *Biochemistry 24*, 1598–1603.
17. Miles, E. W., and Meister, A. (1967) The mechanism of the reaction of β-hydroxyaspartate with L-aspartate β-decarboxylase. A new type of pyridoxal 5′-phosphate-enzyme inhibition. *Biochemistry 6*, 1734–1743.
18. Jenkins, T. (1969) Glutamic-Aspartic Transaminase VI. The Reaction with Certain β-Substituted Aspartic Acid Analogues. *J. Biol. Chem. 236*, 1121–1125.
19. von Stosch, A. G. (1996) Aspartate aminotransferase complexed with *erythro*-β-hydroxyaspartate: Crystallographic and spectroscopic identification of the carbinolamine intermediate. *Biochemistry 35*, 15260–15268.
20. Hayashi, H., and Kagamiyama, H. (1995) Reaction of aspartate aminotransferase with L-*erythro*-3-hydroxyaspartate: Involvement of Tyr70 in stabilization of the catalytic intermediates. *Biochemistry 34*, 9413–9423.
21. Hayashi, H., Mizuguchi, H., and Kagamiyama, H. (1998) The imine-pyridine torsion of the pyridoxal 5′-phosphate Schiff base of aspartate aminotransferase lowers its pK_a in the unliganded enzyme and is crucial for the successive increase in the pK_a during catalysis. *Biochemistry 37*, 15076–15085.
22. Jäger, J., Moser, M., Sauder, U., and Jansonius, J. N. (1994) Crystal structures of *Escherichia coli* aspartate aminotransferase in two conformations. Comparison of an unliganded open and two liganded closed forms. *J. Mol. Biol. 239*, 285–305.
23. Phillips, R. S., Miles, E. W., Holtermann, G., and Goody, R. S. (2005) Hydrostatic Pressure Stabilizes the Open Conformation of *Salmonella typhimurium* Tryptophan Synthase. *Biochemistry 44*, 7921–7928.
24. Phillips, R. S., McPhie, P., Miles, E. W., Marchal, S., and Lange, R. (2008) Quantitative Effects of Allosteric Ligands and Mutations on Conformational Equilibria in *Salmonella typhimurium* Tryptophan Synthase. *Arch. Biochem. Biophys. 470*, 8–19.
25. Phillips, R. S., Miles, E. W., Marchal, S., and Lange, R. (2008) Pressure and Temperature Jump Relaxation Kinetics of *Salmonella typhimurium* Tryptophan Synthase L-Serine Complex Reveal Large Transition State Compressibility and Heat Capacity Changes. *J. Am. Chem. Soc. 130*, 13580–13588.
26. Seifert, T., Bartholmes, P., and Jaenicke, R. (1982) Reconstitution of the isolated β2-subunit of tryptophan synthase from *Escherichia coli* after dissociation induced by high hydrostatic pressure. Equilibrium and kinetic studies. *Biophys. Chem. 15*, 1–8.
27. Kogan, A., Gdalevsky, G. Y., Cohen-Luria, R., Goldgur, Y., Phillips, R. S., Parola, A. H., and Almog, O. (2009) Conformational changes and loose packing promote *E. coli* tryptophanase cold lability. *BMC Struct. Biol. 9*, 65.
28. Kallen, R. G., Korpela, T., Martell, A. E., Matsushima, Y., Metzler, C. M., Metzler, D. E., Morozov, Yu. V., Ralston, I. M., Savin, F. A., Torchinsky, Yu. M., and Ueno, H. (1985) in Transaminases (Christen, P., and Metzler, D. E., Eds.) pp 37−108, John Wiley & Sons, New York.
29. Guex, N., and Peitsch, M. C. (1997) SWISS-MODEL and the Swiss-PdbViewer: An environment for comparative protein modeling. *Electrophoresis 18*, 2714–2723.